JPP Journal of Pharmacy and Pharmacology

JPP 2007, 59: 1473–1484

Received March 26, 2007
Accepted July 31, 2007
DOI 10.1211/jpp.59.11.0003
ISSN 0022-3573

Laser-ablated nanofunctional polymers for the formulation of slow-release powders for dry powder inhalers: physicochemical characterization and slow-release characteristics

Intira Coowanitwong, Vikram Arya, Gina Patel, Won-Seok Kim, Valentin Craciun, James R. Rocca, Rajiv Singh and Günther Hochhaus

Abstract

Recently, dry powder inhalation (DPI) powders coated with nanometre-thin layers of biodegradable polymers, prepared using pulse laser deposition (PLD), have been evaluated as a slow-release formulation for DPI use, with the goal of improving pulmonary selectivity. This paper describes evaluation of the chemical stability of one potential polymer, poly lactic acid (PLA), during the ablation process, the resulting respirable properties and potential cytotoxicity of coated glucocorticoid powders, and the resulting sustained-release characteristics of PLA-coated glucocorticoids creating using PLD. Triamcinolone acetonide (TA) and budesonide (BUD) were used as two model glucocorticoids to determine pulmonary targeting (PT) in-vivo.

The chemical stability of PLA was determined at various laser energy densities. The respirable fraction and the cytotoxicity of the micronized particles of TA and BUD, coated using optimum laser energy density, were determined. In-vitro dissolution profiles were generated for the coated/uncoated formulations and an ex-vivo receptor binding assay was used to determine PT in rats.

Increasing laser energy density led to decreases in molecular weight and film density, and increases in degradation products, roughness and thickness of the film. The mean dissolution time of coated formulations of BUD was longer (4 h) than with the less lipophilic TA (2 h). This correlated well with a more pronounced pulmonary selectivity observed for coated BUD ex-vivo.

Stability and the physical properties of the film correlated with the laser energy density. We observed a direct relationship between the dissolution rate of the uncoated and coated formulation and the degree of PT; however, physiochemical properties of the drug (e.g. lipophilicity) may also contribute to the improved PT.

Department of Pharmaceutics, College of Pharmacy, University of Florida, Gainesville, FL 32610, USA

Intira Coowanitwong, Vikram Arya, Gina Patel, Günther Hochhaus

Department of Material Science and Engineering, College of Engineering, University of Florida, Gainesville, FL 32611, USA

Won-Seok Kim, Valentin Craciun, Rajiv Singh

Advanced Magnetic Resonance Imaging and Spectroscopy Facility (AMRIS), McKnight Brain Institute, University of Florida, Gainesville, FL 32610, USA

James R. Rocca

Correspondence: Günther Hochhaus, Department of Pharmaceutics, College of Pharmacy, University of Florida, Gainesville, FL 32610, USA.
E-mail: hochhaus@cop.ufl.edu

Acknowledgements: The authors acknowledge the financial support of the Particle Engineering Research Center (PERC) for Particle Science and Technology at the University of Florida, The National Science Foundation (NSF Grant EEC-94-02989), and the Industrial Partners of the ERC for support of this research.

Any opinions, findings and conclusions or recommendations expressed in this material are those of the author(s) and do not necessarily reflect those of the NSF.

Introduction

Airway inflammation plays a central role in the pathogenesis of asthma, and anti-inflammatory drugs such as corticosteroids are highly effective in alleviating the symptoms of asthma (Thomson 2004; Barnes 2006). Inhaled corticosteroid therapy is the preferred treatment, as it provides high pulmonary efficacy with low systemic toxicity.

Pharmacokinetic–pharmacodynamic simulations and animal experiments suggest that in order for inhalation therapy to produce optimized pulmonary targeting (PT), it is crucial to have prolonged pulmonary release of the drug (Hochhaus et al 1997; Talton et al 2000; Hochhaus et al 2002). A variety of approaches have been suggested for prolonged pulmonary residence. These approaches include slow dissolution of the drug particles (Hochhaus 2007), corticosteroid esterification in the lung (Miller-Larsson et al 1998), and the use of sustained-release drug encapsulation systems such as liposomes (Suarez et al 1998).

UV laser ablation was introduced in the 1980s (Srinivasan & Mayne-Banton 1982; Srinivasan & Braren 1989) and has found applications in electronics, micromechanics, lithography, and in medicine in the preparation of coatings for stent material (Chrisey & Hubler 1994).

Recently, pulse laser deposition (PLD) has been evaluated for the design of slow-release formulations of inhaled glucocorticoids (Talton et al 2000; Coulen et al 2004; Arya et al

2006). In PLD (Figure 1) a laser beam is used to ablate a biodegradable polymer. The ablated nano-sized plume, when released from the polymer reservoir, slowly covers the surface of the dispersed drug particles with a continuous nanothin film.

Originally, UV laser ablation of polymers was thought to be based on photochemical effects, resulting from photons breaking bonds (Bityurin et al 2003). Effects based on the heating of the polymer by laser (photothermal effects) also have to be considered. The rather complex interaction between laser energy and matter makes it difficult to predict the changes induced on a chemical level (reduction in molecular weight (MW) and induced chemical reactions such as oxidation, reduction and bond breakage).

In this study, we evaluated the properties, chemistry and potential toxicity of the film associated with the laser ablation method for biodegradable polymers, using poly (D, L-lactic acid) (PLA) as a model polymer. We also evaluated the performance of coated particles from differing laser ablation conditions, and the physicochemical properties of the drugs selected for coating.

Materials and Methods

PLA, viscosity 0.55–0.75 dL g^{-1} with an average MW of 75 000–125 000 Da, was acquired from Birmingham Polymers, Inc. (Birmingham, AL, USA). Micronized triamcinolone acetonide (TA) was purchased from PCCA Inc. (Houston, TX, USA). Micronized budenoside (BUD) was obtained from AstraZeneca Pharmaceuticals (Wilmington, DE, USA). Dexamethasone (DEX), methylprednisolone acetate (MPA) and tetrahydrofuran (THF) were obtained from Sigma Chemical Co. (St Louis, MO, USA). 6,7-^{3}H(N) dexamethasone (35–40 Ci $mmol^{-1}$) was purchased from Perkin Elmer Life Sciences (Boston, MA, USA). Dichloromethane-d_2 (CD_2Cl_2) was purchased from Aldrich Chemical Company, Inc. (Milwaukee, WI, USA). Polystyrene standards were purchased from TOSOH Corp. (Minato-Ku, Tokyo, Japan). Extra-fine lactose was donated by EM industry (Hawthorne, NY, USA). Sodium chloride, monobasic sodium phosphate, dibasic sodium phosphate, sodium lauryl sulfate (SDS) and HPLC-grade acetonitrile were purchased from Fisher Scientific (Suwannee, GA, USA). Cytoscint scintillation cocktail was obtained from ICN Biomed (Costa Mesa, CA, USA). Tris/HCl, sodium molybdate, 1, 4-dithioerythritol, and other analytical grade chemicals were obtained from Sigma Chemical Co.

Coating process

The PLD experimental setup is shown in Figure 1. The PLA polymer target was prepared in a Carver Press (Carver, Inc., Wabash, IN, USA). PLA (1 g) was transferred into a 1×0.25 inch circular mould, and then pressed using 2500 psi at 100°C for 10 min. The target was mounted within the vacuum chamber on a motor and rotated during each deposition run, in order to ensure uniform ablation. A krypton–fluoride excimer laser operating at 248 nm with a pulse width of 25 ns was used in the experiments. Deposition was carried out at a base pressure of 1×10^5 torr, with the laser operating at 5 Hz. For polymer stability, PLA was ablated onto flat silicon substrates using laser energy densities of 70, 100, 200, 300 and 500 mJ cm^{-2} for 10 min. For the drug coating, 100 mg of the micronized drug was transferred to the weighing dish, which was attached on the top of a high-speed Vortex-Genie 2T mixer (Fisher Scientific) and positioned within the plume direction. Unless otherwise stated, coating was performed at a laser energy density of 200 mJ cm^{-2} for 1 h.

Chemical stability

Gel permeation chromatography (GPC)

The MW of the PLA was determined by GPC using a Hewlett Packard 1050 pump, HP 1050 autosampler (Hewlett-Packard Co., Santa Clara, CA, USA) with a Shodex RI-71 refractive index detector and Shodex GPC 8 mm ID × 300 cm column (Showa Denka K.K., New York, NY, USA). THF was used as the mobile phase, at a flow rate of 1 ml min^{-1}. The temperature was set at 30°C. Seven polystyrene standards with known narrow MW distributions (1350, 3550, 10 200, 28 000, 87 000, 194 000, 410 000, and 860 000 Da) were dissolved in THF and 100 μL of each solution injected onto the column. The standard MWs (logarithmic) were plotted against retention time to obtain the calibration curve. The as-received and deposited PLA samples were dissolved in THF and purified through a 0.22 μm filter before being injected

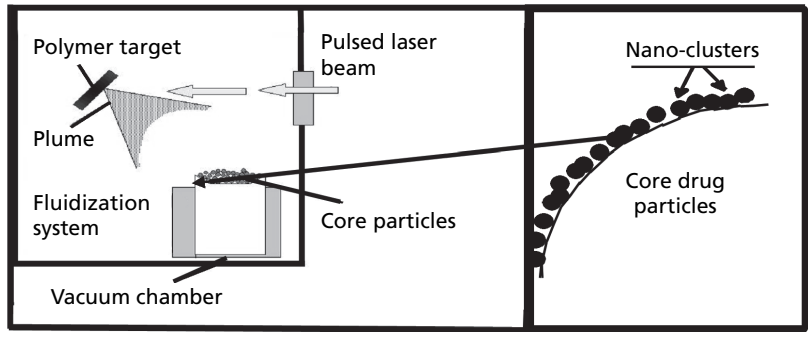

Figure 1 Coating of drug particles by pulse laser ablation of biodegradable polymers.

onto the column. The MW was calculated from the calibration curve using the Millennium software (Waters, Milford, MA, USA).

NMR technique

NMR spectra were recorded on Bruker Advance (DRX) 500 or 600 NMR spectrometers using 5 mm inverse detection with three-channel inverse ($^{1}H/^{13}C/^{15}N$) probes for ^{1}H (1H-NMR, TXI) (Bruker-Biospin Co, Billerica, MA, USA). The as-received and ablated PLA samples were dissolved in CD_2Cl_2 (99.95% ATOM-D). Typically, 500 μL of sample solution was transferred to 5 mm NMR glass tubes. The as-received PLA was also tested as a standard. Chemical shifts were given in parts per million (ppm) relative to $HCDCl_2$ residual at 5.32 ppm.

Typical spectral parameters at 500.4 MHz were: regulated temperature 27°C, pulse angle 60°, spectrum width 6666 Hz (13.3 ppm), acquisition time 4.0 s, time domain size 53 333 points, relaxation delay 1.0 s, and 64–768 scan repetitions. The time domain signal (free induction decay) was processed with 0.25–0.33 Hz exponential line broadening before Fourier transformation to 64 K real data points. The quantitative experiment for degradation products was performed using hexamethyldisiloxane (HMDSO) as an internal standard; 10 μL HMDSO (30 μg mL^{-1}) was added to the solution of PLA ablated with the maximum laser energy density (500 mJ cm^{-2}). The concentration of the degradation products was calculated using equations 1 and 2:

$$M(H)_{unk} = M(H)_{STD} \times [I(H)_{unk} / I(H)_{STD}]) \quad (1)$$

$$C(H)_{unk} = C(H)_{STD} \times [I(H)_{unk} / I(H)_{STD}]) \quad (2)$$

where $M(H)_{unk}$ and $M(H)_{STD}$ are the number of moles of H (hydrogen) atoms in an unknown and the HMDSO standard (18) respectively, $I(H)_{unk}$ and $I(H)_{STD}$ are the signal intensity (area under the peak) of an unknown sample and the standard sample, respectively, and $C(H)_{unk}$ and $C(H)_{STD}$ are the concentrations of H atoms in an unknown sample and the standard, respectively.

Characterization of thin films

X-ray reflectometry (XRR)

The thickness, roughness and density of the polymer layers deposited on the silicon substrate was investigated by XRR using a Panalytical X'Pert MRD system (ALMELO, the Netherlands). The acquired spectra were simulated using the WinGixa software from Panalytical. The roughness of the film is one of the parameters within the simulation. Typically the roughness increase is the 'noise' in the XRR spectra. The roughness of the films was determined by simulation of the spectra and was expressed as a valley-to-peak estimate.

X-ray photoelectron spectroscopy (XPS)

The thickness of the polymer film on drug particles was measured using XPS. The experiment was performed only on TA, since it contains a fluorine group that could come only from the drug and not from contaminants, in addition to carbon and oxygen atoms present on the surface of any sample analysed by XPS. The study was performed in a Kratos analytical surface analyser XSAM 800 (Manchester, UK) using non-monochromatic MgKα radiation (1253.6 eV). Medium-resolution wide scans in the binding energy scale (0–1200 eV) at 50 eV analyser pass energy were collected to identify the elements present. High-resolution narrow scans at 20 eV and 0.1 eV per channel pass energy and 100 ms dwell time were collected for C1s, O1s and F1s XPS peaks to identify their chemical status. The thickness (x) of the coated formulations was estimated using the equation:

$$I = I_0 \exp(-x/\lambda) \quad (3)$$

where I is the signal of fluorine obtained from the coated TA formulation, I_0 is the signal of fluorine in the uncoated TA and λ is the electron escape length (~1.8 nm). Preliminary experiments for BUD and TA looked at different ablation conditions with varying ablation times and energy densities (100, 200 and 300 mJ cm^{-2}).

Dissolution

Samples (10 mg) of uncoated and polymer-coated TA and BUD (equivalent to 10 mg of the uncoated drug) were weighed. PBS (1 L; pH 7.4) was used as the dissolution medium. SDS (0.05%) was added to simulate the pulmonary environment in-vivo. The dissolution apparatus II (Vankel Technology Group, Cary, NC, USA) was operated at a speed of 40 rpm (and in some experiments 10 rpm, see results). Aliquots (1 mL) of the sample were withdrawn at 0, 1, 5, 10, 15, 30 and 45 min and 1, 1.5, 2, 3, 4, 6, 8, 10, 12, 22 and 24 h through a syringe filter unit (filter size 0.2 μm). The aliquot was replaced with an equal volume of the dissolution media to maintain constant dissolution conditions. At the end of the experiment, a sample of the remaining dissolution medium was taken to document mass balance. This was the case in all release experiments.

The withdrawn samples were analysed by HPLC. The percentage of undissolved drug was plotted as a function of time, and the mean dissolution time (MDT) was calculated as the ratio of area under the first moment curve and the area under the curve (AUMC/AUC). The difference in the MDT between coated and uncoated material was used to quantify the degree of slow release. The difference in MDT of the formulations were tested for significance using analysis of variance (Design Expert Version 6 Software for Experiment Design, Stat Ease Inc, Minneapolis, MN, USA) at $\alpha = 0.05$.

Respirable fraction

An eight-stage cascade impactor (Thermo-Andersen Inc., Smyrna,. GA, USA) with a human 'throat' was used to determine the respirable fraction of coated and uncoated material. Three doses (2% drug powder in extra-fine lactose) were loaded into the chamber using an Aerolizer inhaler demonstration unit (Novartis Pharma AG, Basle, Switzerland), with an inspiration rate of 28.3 L min^{-1} (confirmed by a flow meter, Bios International, Butler, NJ, USA) for an inhalation time of 1 min. After each run, the powders on each plate and throat piece of the impactor were collected by rinsing the

plates with 10 mL methanol. HPLC was used to determine the percentage of drug deposited at each stage. Cut-off aerodynamic size ranges for stage 0 to stage 7 are 9.0–10, 5.8–9.0, 4.7–5.8, 3.3–4.7, 2.1–3.3, 1.1–2.1, 0.7–1.1 and 0.4–0.7 μm, respectively, and were taken from the purchase certificate of the impactor. The percentage of the total dose collected from stages 2–5, representing particles with an aerodynamic diameter of 1.1–5.8 μm, was considered to be the respirable fraction.

Cytotoxicity in healthy lung macrophages

In order to determine whether the nanothin coatings had any associated toxicity, the MTT assay was performed using J774A.1 full-adherent murine alveolar monocyte macrophage cells. Cells were grown in a DMEM supplement medium with 10% fetal bovine serum without antibiotics, at 37°C and 5% CO_2. Macrophages were first seeded into 96-well plates (Becton-Dickinson Labware, Franklin Lakes, NJ, USA) at 1×10^5 cells per well, and allowed approximately 24 h to recover. Different concentrations (1000, 100, 10, 1, 0.1 and 0.01 μg mL^{-1}) of the free and polymer-coated drugs, dissolved in culture media, were added. After 24 h incubation, 25 μL MTT solution (5 mg mL^{-1} in PBS) was added to each well. After 3 h incubation with MTT solution, the supernatant was removed and 200 μL DMSO was added to each well. The purple formazan crystals resulting from the test were dissolved completely using a plate shaker for 30 min. The absorbance was measured using a microplate spectrophotometer (Spectramax 250, Molecular Devices, Sunnyvale, CA, USA) at a wavelength of 570 nm.

HPLC of glucocorticoids

The HPLC system consisted of a Perkin Elmer Series 3B pump and a Waters C_{18} (5 cm × ID 4.6 mm) column connected to a Perkin Elmer ISS 100 autoinjector. The detector was a Milton Roy SM-4000 (Milton Roy, Ivyland, PA, USA) attached to a Hewlett Packard HP-3394A integrator. The eluent was monitored at 254 nm. The mobile phase for TA was 30:70 acetonitrile:water plus 0.03% trifluoroacetic acid; the mobile phase for BUD was 60:40 methanol:water. Mobile phases were delivered at a flow rate of 1.0 mL min^{-1}. MPA was added as the internal standard for both drugs. The standard curve was linear in the range of 1–50 μg mL^{-1} ($r^2 > 0.999$). The calibration curves were used to estimate the concentrations of drugs in the dissolution studies. The quality control samples (5, 20, 50 μg mL^{-1}) were always in the range of 80–125%.

In-vivo evaluation of glucocorticoid receptor occupancy

Animal procedures

All animal procedures were approved by the Institutional Animal Care and Use Committee (IACUC), University of Florida. Adult Fischer rats (F-344) weighing 220–250 g were obtained from Harlan Sprague Dawley Inc. (Indianapolis, IN, USA). The rats were housed in a constant temperature environment with a 12-h light/dark cycle before the experiment. They were fed a standard pellet diet and water as required, but were food-fasted overnight before each experiment.

Drug administration procedure

The anaesthetic was a mixture of 1.5 mL ketamine 10%, 1.5 mL xylazine 2% and 0.5 mL acepromazine 1%, given subcutaneously in a volume of 1 mL kg^{-1}. The depth of anaesthesia was checked using the tail-pinch or pedal-withdrawal reflex. For intratracheal administration, 1 inch of a special round-tipped canula attached to a delivery device for administration of dry powders (Penn-Century, Philadelphia, PA) was introduced into the trachea via the mouth. Uncoated and coated dry-powder drugs were diluted to 0.4% using extra-fine lactose. Approximately 5 ± 0.5 mg of powder (equivalent to 100 μg kg^{-1} of bodyweight of rats used in the subsequent experiments) was placed in the device and instilled into the lungs with insufflations of 3 mL air. Extra-fine lactose was administered as a placebo. Rats were decapitated at 1, 2.5 and 6 h, and the tissues (lung and liver) were removed and immediately processed for receptor binding studies.

Ex-vivo receptor binding assays

A previously developed ex-vivo receptor binding assay was used (Suarez et al 1998). Immediately after removal, the tissue (lung or liver) was weighed and placed on ice. Tissue was homogenized with 4 volumes (for lung) or 10 volumes (for liver) of ice-cold incubation buffer (10 mM Tris/HCl, 10 mM sodium molybdate, 2 mM 1,4-dithioerythritol) and 2mL of the homogenate was incubated with 5% charcoal (in cold distilled water) for 10 min to remove unbound corticosteroids. The homogenate was centrifuged (20 min at 20 000g, 4°C) in a Beckman (Fullerton, CA, USA) ultracentrifuge equipped with a JA-21 rotor to obtain a clear supernatant. Aliquots of the supernatant (150 μL) were added to pre-chilled microcentrifuge tubes containing 50 μL of either 25 nM 6,7-^{3}H (N) DEX for determination of total binding or a mixture of 25 nM 6,7-^{3}H (N) DEX and 25 μM unlabelled DEX for determination of non-specific binding. The tubes were vortexed and incubated at 4°C for 18 h.

After 18 h, 200 μL of activated charcoal (5% in ice-cold distilled water) was added to the microcentrifuge tubes to remove excess radioactivity. The microcentrifuge tubes were vortexed, centrifuged for 5 min, and 300 μL of the supernatant was removed and added to the scintillation vial, to which 5 mL scintillation cocktail (Cytoscint) was added. Vials were read in a scintillation counter (Beckman, LS 5000 TD, Palo Alto, CA, USA) to obtain the radioactive counts (dpm).

For each tissue (lung or liver), the area under the free receptor vs time profile was calculated over the 6 h time period ($AUEC_{0–6h}$) using the trapezoidal rule. $AUEC_{0–6h}$ of 0% × h indicated full receptor occupancy; 600% × h indicated no receptor occupancy. Data are based on three or four independent experiments (three or four animals per time point).

Statistical analysis

Pulmonary and hepatic receptor occupancy at individual time points for all animals included in a given experiment subset (liver and lung receptor occupancy for uncoated and coated formulations) were compared using analysis of variance

(using SigmaStat, Systat, San Jose, CA, USA), as data showed normal distribution with equal variance. Statistical significance was assumed for $P < 0.05$. Multiple comparison was performed using the Holm–Sidak test.

To quantify differences in receptor occupancy between pulmonary and hepatic receptors, the cumulative change from the 100% baseline (AUEC) was calculated for the 6-h investigation period using the trapezoidal rule from percent free receptor vs time profiles. In accordance with previous publications (Hochhaus et al 1997; Arya et al 2006), PT was defined as the difference between AUEC for lung and liver. This method was preferred over the ratio, as previous studies using a range of doses showed that the optimal selectivity ratio was obtained for the dose approaching zero (Hochhaus 1997). Using the difference therefore represents a more meaningful parameter.

Results and Discussion

Nanothin polymer coating around micronized particles created using a laser ablation technique might be a promising approach for the design of slow-release inhalation devices. Within this context, it was of interest to characterize the suitability of this method in therapeutic applications. We therefore evaluated the chemical stability of a model polymer during ablation, assessed the respirable behaviour of the engineered particles, determined the potential cytotoxicity of the material, and related the sustained-release characteristics of PLA-coated powders to ablation conditions and tried to relate these to the achieved effect on pulmonary selectivity.

Chemical stability

Gel permeation chromatography

The effect of the laser energy density (mJ cm^{-2}) on the resulting MW of PLA revealed that the ablation process led to a significant reduction in MW. After applying laser energy densities of 70, 100, 200, 300 and 500 mJ cm^{-2}, the MW of PLA was significantly reduced from 77 500 Da (MW of authentic PLA) to 39 800, 8300, 2600, 2600 and 8600 Da, respectively. The results suggest that an increase in laser energy density (i.e. 70 to 200 mJ cm^{-2}) led to a higher degree of polymer breakdown, resulting in a decrease in MW. The breakdown of the PLA started from 70 mJ cm^{-2} and the maximum breakdown was found at 200 mJ cm^{-2}. Increasing the laser energy-density to 300 mJ cm^{-2} had no effect on MW. However, a slightly elevated MW was detected at 500 mJ cm^{-2} (8600 Da).

Figure 2A shows the GPC chromatogram of authentic PLA, indicating a normal distribution of the MW. By

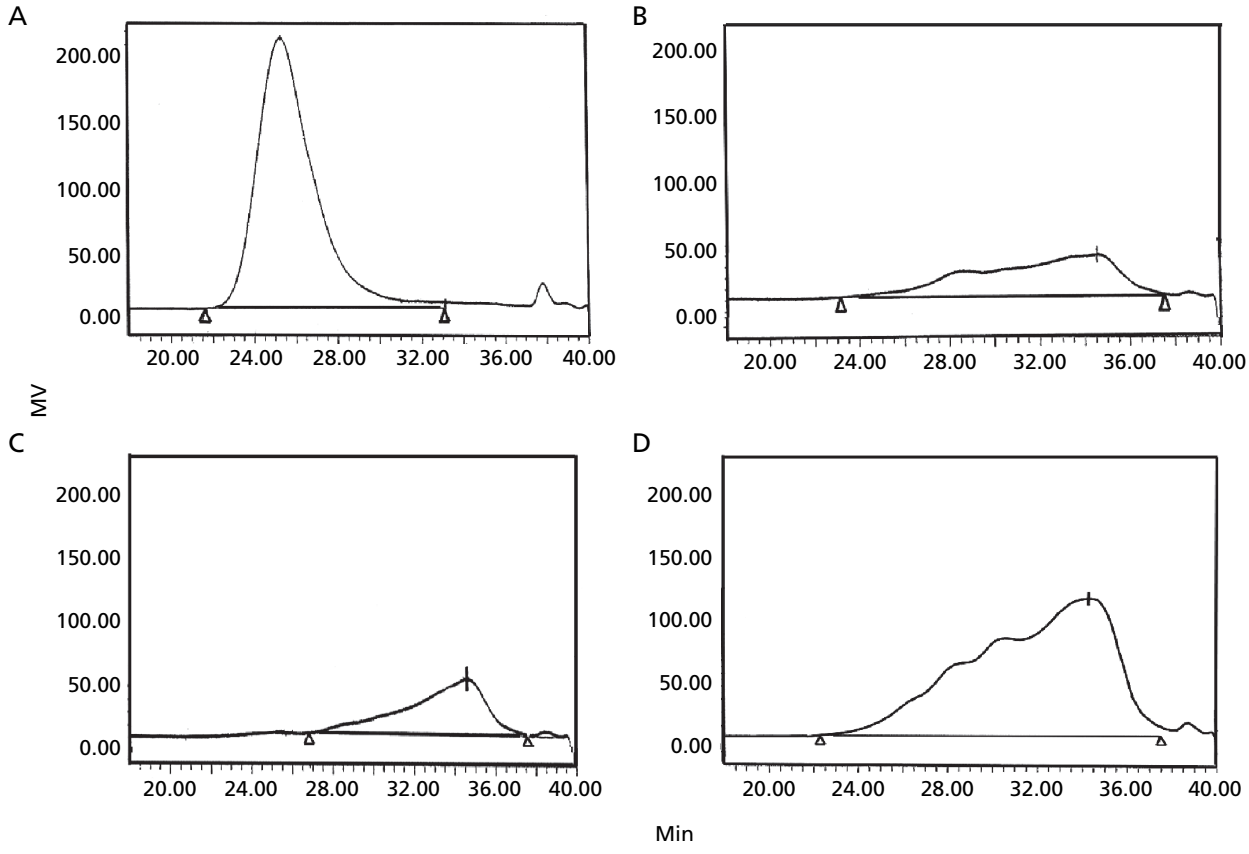

Figure 2 Gel permeation chromatogram of as-received poly lactic acid (PLA) (A) and PLA ablated by 100 (B) 300 (C) and 500 (D) mJ cm^{-2}.

converting elution times to the polymer MW (i.e. by comparing them with the polystyrene standard curve), the MW distribution of the authentic PLA was found to be within the range 396 700–447 Da (average MW 77 500). Figures 2B–D show examples of GPC chromatograms of deposited PLA obtained from low, medium and high laser energy densities (100, 300 and 500 mJ cm^{-2}). The figures show an irregular peak shape of MW distribution, and the MW were found within the range 163 700–36 Da for 100 mJ cm^{-2}, 19 000–32 Da for 300 mJ cm^{-2} and 29 500–400 Da for 500 cm^{-2}. These results indicate that an increase in laser energy density led to a shift toward the lower range of the MW distribution. Suzuki et al reported a similar result in the case of silicon-based polymers, where the molar mass distribution was dependent on the energy density (Suzuki et al 2000). The ablated films showed a molar mass reduction and a broader distribution compared with the authentic polymer (Figure 2). The relationship between MW of deposited PLA and the laser density is in agreement with bond breakage induced by UV radiation. The slight increase in MW at the highest laser density may be due to the mechanical removal of the polymer chunks as a result of the coating process. Similar results in obtaining polymer fragments and clusters after ablation with high laser energy densities have been reported by Rau (2002). Similar conclusions could be drawn from the actual GPC chromatograms, which showed a shift from a normal distribution for non-ablated material to a more skewed MW distribution for ablated material. The hypothesis, that at higher laser densities higher MW material ('chunks') are removed, is supported by the chromatograms. Such conditions might be useful if higher MW depositions are desired. The distinct reduction in MW might actually be an advantage for the pulmonary delivery of such formulations, as this would allow the absorption of polymer from the lung into the systemic circulation, and opens the possibility of renal elimination, while inhalation of large quantities of high MW polymers might result in pulmonary accumulation. Indeed, low MW oligolactic acid has been used in aerosol formulations for inhalation without any toxicity (Leach 2007).

NMR

NMR was used to identify the possible degradation products of the polymer formed in the process of laser ablation. The ^{1}H-NMR spectra of the authentic and ablated PLA for different laser energy densities are shown in Figure 4 (A–F). The CD_2Cl_2 solvent shows a residual ^{1}H signal at 5.32 ppm, while the as-received PLA provided a signal for CH at 5.2 and for CH_3 at 1.5 ppm. CD_2Cl_2 was selected for this study because PLA is highly soluble in this solvent and because the signal of this solvent showed no interference with the PLA signals (Sodergard & Stolt 2002). Compared with the authentic PLA spectrum (Figure 3A), the results of ablated film (Figure 3B–F) showed the appearance of new peaks, implying the formation of new chemical functional groups as a result of the ablation process. With an increase in laser energy density, the signal intensities of new products increased. The possible degradation products could be identified from the chemical shift of standard substances reported by Abraham & Loftus (1978) and Silverstein & Webster (1991): acids 2–2.6 ppm, esters 2–2.2 ppm, vinyl 3.8–7.9 ppm, aldehydes 9–10 ppm.

By considering possible degradation processes (Figure 4), some of the new products appeared to be alkenes and aldehydes. In an attempt to identify the new degradation products, relevant authentic samples of acrylic acid and acrolein were analysed and the spectra compared with the spectra of laser-ablated material. Figure 5 shows that acrylic acid and aldehydes were clearly formed. Formation of aldehydes is of particular concern because these are toxic to the respiratory tract. The severity of aldehyde toxicity ranges from irritation at low concentrations to pulmonary oedema at high concentrations (Environmental Protection Agency (EPA), National Institute for Occupational Safety and Health Registry of Chemical Substances (NIOH)). A quantitative NMR experiment showed that the amount of aldehydes was 0.053 μg per dose of rifampin (600 μg), which was significantly lower than the toxic range (3100 μg per 6 h per 2 weeks intermittently) as determined by the NIOH. Aldehyde generation might be reduced by more rigorous removal of oxygen from the ablation chamber.

X-ray reflectometry and X-ray photoelectron spectroscopy

XRR analysis was performed on films deposited on silicon substrates, a structure much simpler to analyse and model than coated particulates. Two laser energy densities (150 and 300 mJ cm^{-2}) were used to study the effect of laser energy density on the thickness, density and roughness of the films. Acquired and simulated XRR spectra are shown in Figure 6. The simulation results for the film deposited by a laser energy density of 150 mJ cm^{-2} indicated a thickness of 20 nm, a density of 1.45 g cm^{-3} and a roughness of 13 nm; values of 0.52 g cm^{-3}, 180 nm and 40 nm, respectively, were found for the film deposited by a laser energy density of 300 mJ cm^{-2}. Although only two levels of laser energy density were used for this study, it was obvious that the film deposited using the higher laser-density energy had a lower density but higher roughness and thickness compared with the film coated with the lower laser energy density. The use of a higher laser energy density might therefore be of advantage if a more pronounced coating needs to be achieved. On the other hand, the resulting coatings were rougher, favouring agglomeration of the material produced.

The thickness of the applied polymer film after PLD was determined using XPS. The experiment was performed only on TA since it contains a fluorine group that could come only from the drug and not from contaminants, in addition to carbon and oxygen atoms which are present on the surface of any sample analysed by XPS. By monitoring the intensity of the F1s peak by XPS it is possible to estimate the thickness of the polymer film on the drug particles. XPS spectra of free and coated particles by laser energy density of 300 mJ cm^{-2} showed a clear reduction of the F1s signal for the coated material, which indicated an average coating thickness of approximately 1 nm (data not shown). This is somewhat thinner than achieved by infrared (Bubb et al 2004).

The nanothin nature of these coatings was also confirmed by testing the drug content of coated material using reverse-phase

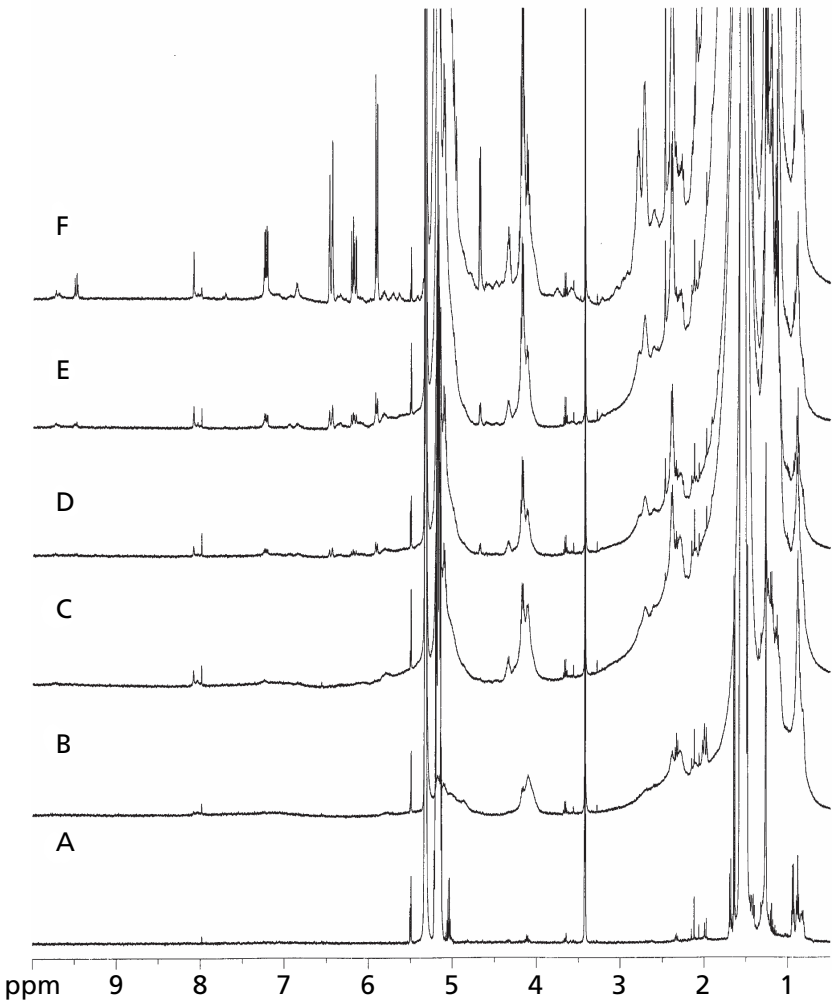

Figure 3 NMR spectra of authentic poly lactic acid (PLA) (A) and PLA ablated using laser energy densities of 70 (B), 100 (C), 200 (D) 300 (E) and 500 (F) mJ cm^{-2}.

HPLC. For both TA and BUD, drug content on a weight/weight basis were indistinguishable from pure drug and was within the standard error of the assay (<2%) using ablation times of 30 and 50 min.

In-vitro dissolution test

Material coated at 200 mJ cm^{-2} showed the slowest release behaviour. However, there were significant differences in the dissolution behaviour of material collected from the top and bottom of the fluidization bed, with a slower dissolution observed for material collected from the top. This indicated poor mixing of the powders by the mixing device. After improvement of the fluidization process using the method described in the Method section, BUD and TA were coated at 200 mJ cm^{-2}. Figure 7A shows the dissolution profiles of uncoated and coated TA. Both release profiles show a mono-exponential decline in the percentage of undissolved drug. The dissolution of the uncoated and coated TA was complete at 6 and 8 h, respectively. The MDT was 1.2 ± 0.5 h for uncoated TA and 2.0 ± 0.7 h for coated material; thus, the differences between coated and uncoated TA were relatively small. More pronounced differences in the dissolution profile of coated and uncoated TA were obtained under milder conditions (lower surfactant concentration and slower paddle speed, see below).

The dissolution profiles for BUD, using conditions identical to those used for TA in Figure 7A, are shown in Figure 7B. The uncoated drug was completely dissolved within 4 h, with a mono-exponential dissolution profile. The bi-exponential profile for the coated material indicated a burst effect of about 50% (at early time points); about 10% of the dose did not dissolve during the 24-h time period. The MDTs for the uncoated and coated formulations were 1.2 ± 0.5 and 4.7 ± 0.1 h, respectively (not considering the 10% undissolved material). Dissolution profiles for coatings generated at 200 mJ cm^{-2} and 300 mJ cm^{-2} laser densities were similar.

These experiments showed that both steroids dissolved quickly, with similar mono-exponential dissolution profiles. Considering the relatively high surfactant concentrations used

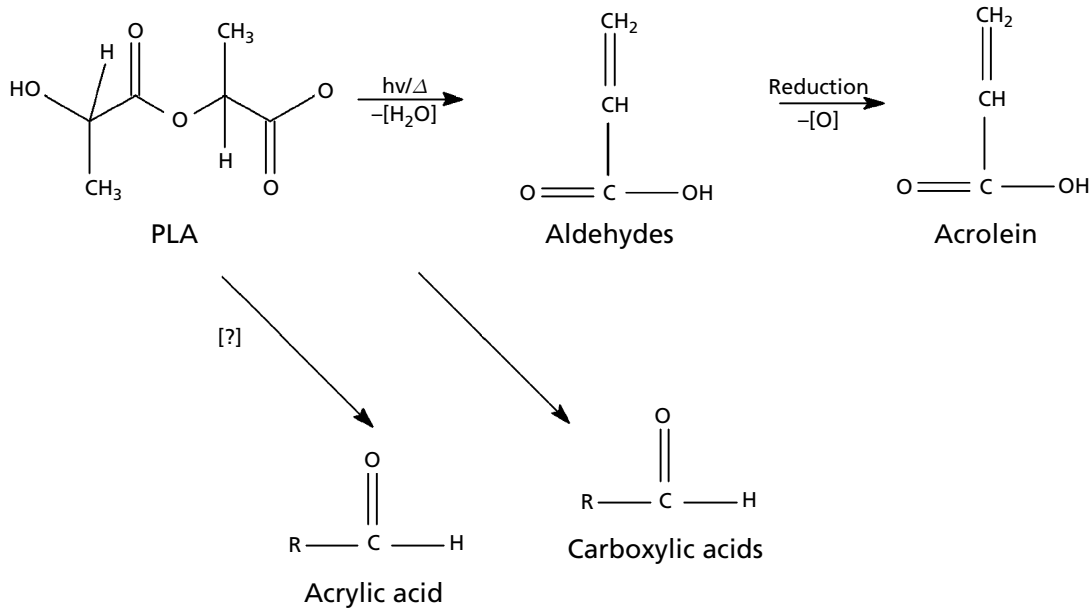

Figure 4 Possible degradation processes of poly lactic acid after pulse laser deposition.

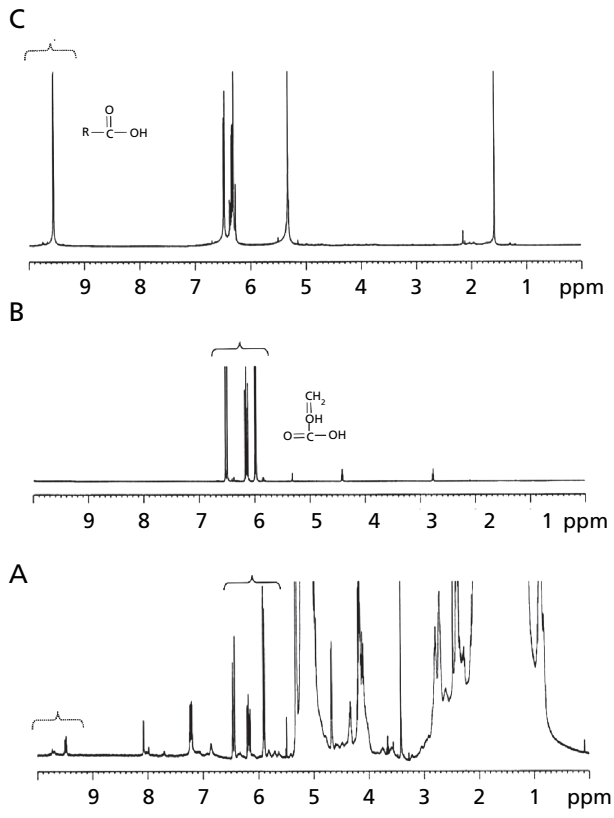

Figure 5 NMR spectra of ablated poly lactic acid (PLA) (A), acrylic acid (B) and acrolein (C).

under distinct sink conditions, the result was to be expected, especially given the similarities in aqueous solubility of the compounds.

Dissolution tests for the polymer-coated TA showed a minor prolongation in the dissolution rate compared with uncoated drug (1.2 vs 2.0 h). However, distinct differences were seen between the dissolution profiles of the uncoated and the polymer-coated BUD (1.2 vs 4.0 h). Coated BUD displayed biphasic drug release characteristics. In the first phase, the 'burst effect' occurred within 4 h, followed by a second slower phase that could be prolonged for more than 24 h. The first phase might be attributed to release of drug from superficial areas of the coated particles, and might have involved only dissolution of uncoated material, while the second phase of release could be attributed to diffusion of the drug through channels in the continuous film of the polymer.

Because the ablation conditions were identical, only the physicochemical differences between the BUD and TA powders could be responsible for the differences in dissolution in-vitro. One might hypothesize that the more lipophilic properties of BUD (as indicated by its longer retention time observed in reverse-phase HPLC) permitted a more intense bonding between polymer and drug particles, and a slower rate of dissolution. However, differences in the structure of the solid particles, for example in morphous character, density and crystal structure, might also be relevant. This would suggest that for drugs such as TA, thicker or more complete coatings are necessary. Although other experiments with hydrophilic drugs such as rifampin (data not shown) seem to support the hypothesis of a relationship between the lipophilicity of a drug and the ability to sustain release of the drug by using polymer coatings, further studies to investigate the actual events at the drug–polymer interface are warranted.

Particle size distribution, respirable fraction

Particle size distributions of coated and uncoated TA and BUD formulations are shown in Figure 8. The respirable

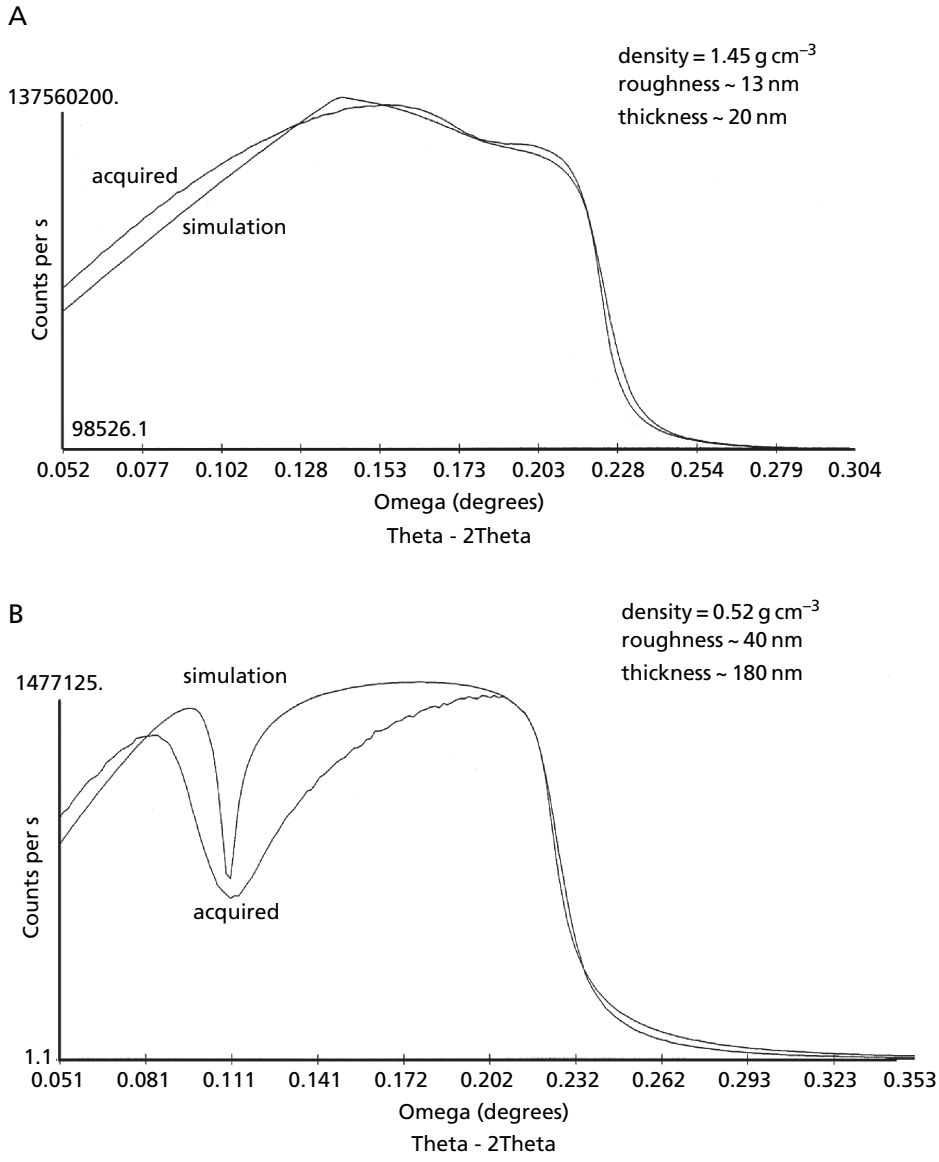

Figure 6 Acquired X-ray reflectometry spectra and simulation of deposited silicon polymer on silicon wafers using 150 (A) and 300 (B) mJ cm^{-2}.

fractions (stages 2–5) of the free and coated formulations were not significantly different, which is in good agreement with the XPS results where exceptionally thin film was being coated onto the particles (1 nm). A larger amount of BUD was found on stage 0, indicating that the overall size distribution might have differed between coated TA and BUD. These fractions would need to be broken up if commercial use is intended. Alternatively, improvement of the powder fluidization would prevent this agglomeration. The reason for BUD showing more agglomeration needs further investigation. However, it might contribute in part to the release profile seen for BUD.

In order to investigate whether just the difference in size (e.g. due to agglomeration) explains the difference in the sustained release characteristics, coated and uncoated TA material was collected from different stages of the cascade impactor, and the dissolution behaviour was assessed under less stringent conditions (lower surfactant concentration, slower paddle speed). Larger particles obtained from stages 0–2, (4.7–10 μm) showed a slower dissolution profile than corresponding uncoated material. Similarly, smaller coated particles (obtained from stages 3–5 (1.1–4.7 μm) released the drug more slowly than uncoated drug of the same size distribution. Thus, the coating process is the driving force for the drug release within a defined particle-size window.

Cell toxicity

Pulmonary macrophage cell cultures were viable for both coated BUD and coated TA over the concentration range 0.1 $\mu g\,mL^{-1}$ to 1 $mg\,mL^{-1}$. The viability curves were superimposable for coated and uncoated material, indicating no toxicity. These results are in agreement with the lack of toxicity

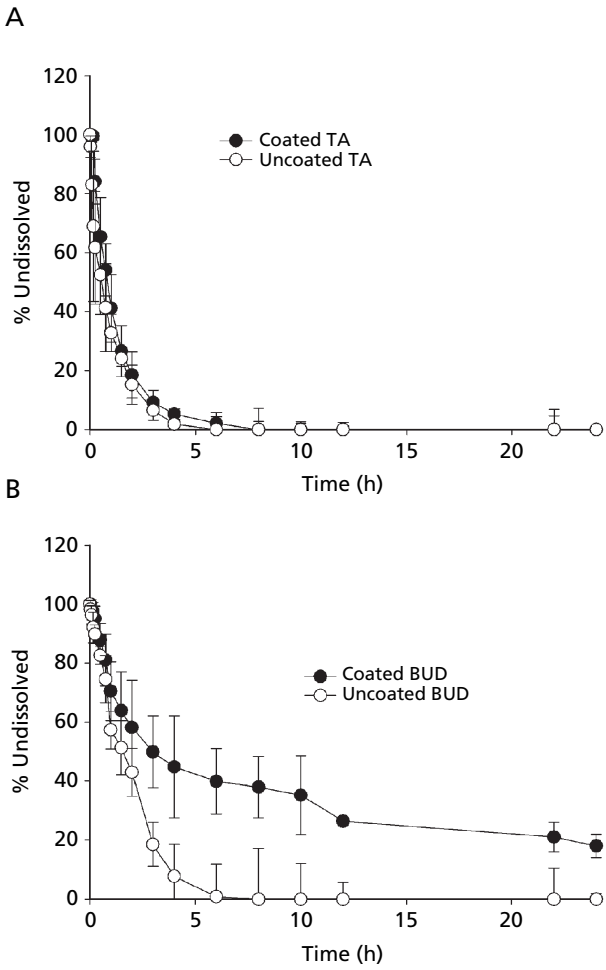

Figure 7 Dissolution profiles of triamcinolone acetonide (TA) (A) and budenoside (BUD) (B) dry powder in pH 7.4 phosphate-buffered saline at 37°C.

reported for oligolactic acid in inhalation aerosol formulations (Leach 2007).

Ex-vivo receptor binding assays

A validated ex-vivo receptor binding assay was used to compare the PT of the two preparations prepared under identical conditions. The receptor occupancy vs time profiles after intratracheal administration of uncoated and coated TA powders are shown in Figure 9A and B. Table 1 compares the AUEC and PT of uncoated and coated formulations of TA and BUD. Analysis of variance comparing the receptor occupancy data indicated significant differences among the groups. Holm–Sidak tests showed no significant difference in receptor occupancies between lung and liver for coated and uncoated formulations of TA. Figure 9C and D show the receptor occupancy vs time profiles after administration of uncoated and coated BUD. For uncoated BUD there was no significant difference in receptor occupancy between lung and liver, whereas for the coated powder there was a significant difference in receptor occupancy between lung and liver ($P < 0.05$).

These results show no significant differences in PT of uncoated TA and BUD or between uncoated and coated TA. However, a significant difference in PT was found between the uncoated and coated BUD ($P < 0.05$).

The results indicate that slower dissolution of coated BUD translated into an increase in pulmonary selectivity. This finding agrees with the pharmaokinetic–pharmacodynamic-based hypothesis that a reduction in the release rate improves lung selectivity. In addition, the receptor binding results for the uncoated formulations agreed well with the in-vitro dissolution profiles, which showed immediate dissolution with the uncoated formulation. This fast in-vitro dissolution suggests rapid absorption from the lung into the systemic circulation, resulting in minimal pulmonary selectivity. In the case of coated TA, although the polymeric coatings provided a slower dissolution rate under less stringent conditions, it was not sufficient

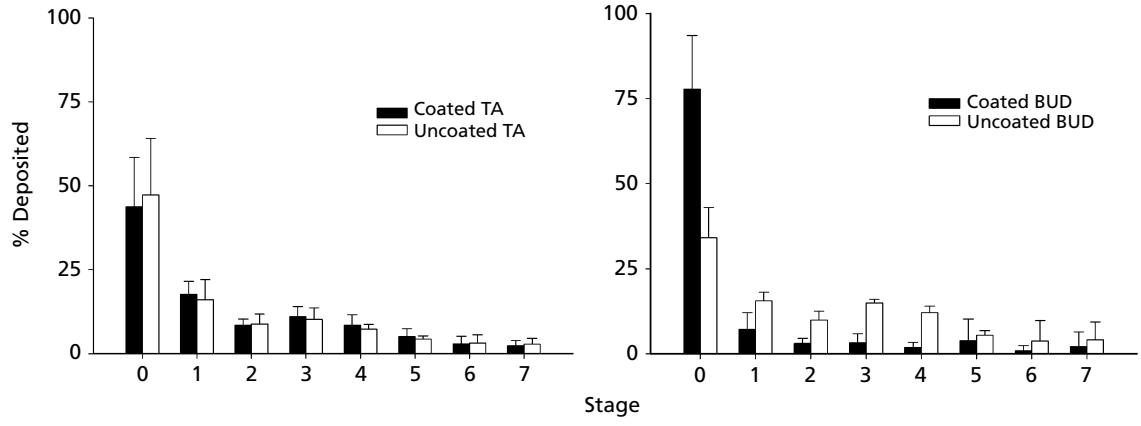

Figure 8 Determination of respirable fraction for coated and uncoated triamcinolone acetonide (TA; left) and budesonide (BUD, right). The percentage of the total dose collected from stages 2–5, representing particles with an aerodynamic diameter 1.1–5.8 μm, was considered as the respirable fraction.

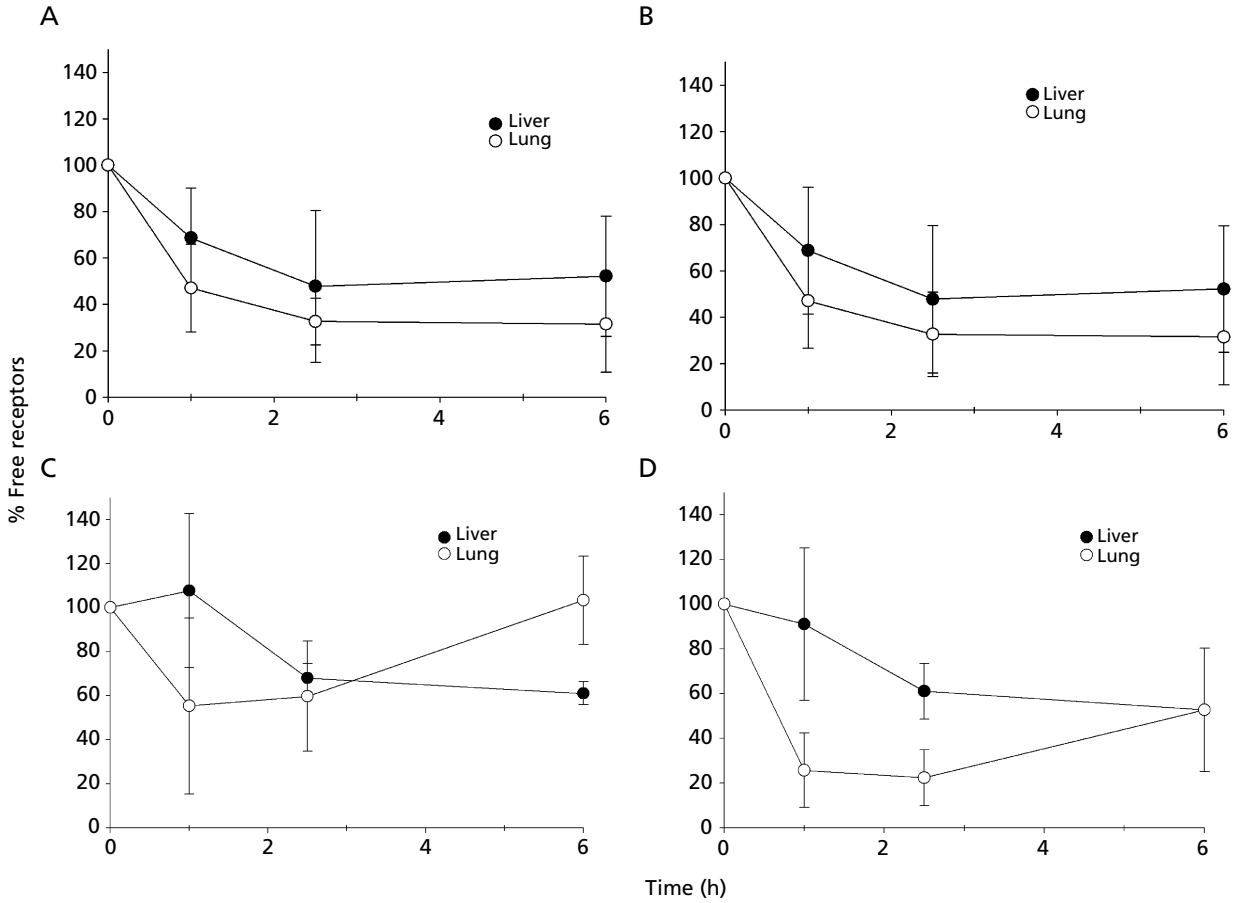

Figure 9 Receptor occupancy vs time profile after the administration of uncoated (A) and coated (B) triamcinolone acetonide formulations and uncoated (C) and coated (D) budenoside formulations in lung and liver tissue.

Table 1 Comparison of area under the effect curves (AUEC) and pulmonary targeting (PT) of uncoated and coated formulations of triamcinolone acetonide (TA) and budenoside (BUD). PT is the difference between the AUEC for lung and liver

	TA		**BUD**	
	Uncoated	Coated	Uncoated	Coated*
$AUEC_{Lung}$ (%×h)	354.4 ± 101.1	299.5 ± 191.9	166.6 ± 53.5	367.6 ± 29.4
$AUEC_{Liver}$(%×h)	253.4 ± 156.8	226.9 ± 160.1	159.5 ± 18.3	199.9 ± 73.8
PT	101.0 ± 60.2	89.6 ± 97.1	23.8 ± 41.3	167.7 ± 45.0

*Differences between $AUEC_{Lung}$ and $AUEC_{Liver}$ were significant ($P < 0.05$).

to show differences in PT in-vivo. In the case of coated BUD, there were significant differences in the in-vitro dissolution rate and receptor occupancies between the lung and liver, which indicates significant pulmonary selectivity. In summary, our results confirm a relationship between the in-vitro dissolution characteristics of the uncoated/polymer-coated drug powders, and the degree of pulmonary selectivity. Differences between results observed for coated TA and BUD seem to indicate that control of the release rate depends on the physicochemical characteristics of the drug, such as the degree of lipophilicity or other solid characteristics (e.g. porosity, density, crystal structure).

Conclusions

This study showed that laser ablation of PLA reduces the MW of the polymer, and generates breakdown products such as alkenes and aldehydes, particularly at higher laser energy density. The concentrations generated are too low to be toxic,

however. In addition, the results suggest that physicochemical differences between the selected drug candidates affect the dissolution rate and PT of PLA-coated dry powders of inhaled glucocorticoids, as BUD showed a distinct increase in MDT and pulmonary selectivity compared with TA. Future studies should focus on optimizing the coating conditions in order to improve the pulmonary selectivity of a wide range of drugs.

References

Abraham, R. J., Loftus, P. (1978) *Proton and carbon-13 NMR spectroscopy, an integrated approach*. Heydon, London

Arya, V., Coowanitwong, I., Brugos, B., Kim, W. S., Singh, R., Hochhaus, G. (2006) Pulmonary targeting of sustained release formulation of budesonide in neonatal rats. *J. Drug Target* **14**: 680–686

Barnes, P. J. (2006) How corticosteroids control inflammation: Quintiles Prize Lecture 2005. *Br. J Pharmacol*. **148**: 245–254

Bityurin, N., Luk'yanchuk, B. S., Hong, M. H., Chong, T. C. (2003) Models for laser ablation of polymers. *Chem. Rev*. **103**: 519–552

Bubb, D. M., Toftmann, B., Haglund, R. F., Horwitz, J., Papantonakis, M., McGill, R., Wu, P. W., Chrisey, D. (2004) Resonant infrared pulsed laser deposition of thin biodegradable polymer films. In: Chrisey, D. B., Eason, R. (eds) *Pulsed laser deposition of thin films: Applications in electronics, sensors, and biomaterials*. John Wiley & Son, New York.

Chrisey, D., Hubler, G. (1994) *Pulse laser deposition*. John Wiley & Son Inc, New York

Coulen, H., Hughes, J., Talton, J., Hochhaus, G. (2004) A novel method for polymer coating of plasmid DNA: initial investigations into the use of pulse laser deposition and gene delivery. *J. Drug Target* **12**: 237–241

Hochhaus, G. (2007) What pharmacokinetic and pharmacodynamic properties are important for inhaled glucocorticoids? *Ann Allergy Asthma Immunol*. **98**: S7–S15

Hochhaus, G., Mollmann, H., Derendorf, H., Gonzalez-Rothi, R. J. (1997) Pharmacokinetic/pharmacodynamic aspects of aerosol therapy using glucocorticoids as a model. *J. Clin. Pharmacol*. **37**: 881–892

Hochhaus, G., Derendorf, H., Talton, J. (2002) Factors involved in the pulmonary targeting of inhaled glucocorticoids. The use of pharmacokinetic/dynamic stimulation. In: Schleimer, R., O'Byrne, P., Szefler, S., Brattsand, R. (eds) *Inhaled steroids in asthma*. Marcel Dekker, New York, pp 283–307

Leach C. (2007) Inhalation aspects of therapeutic aerosols. *Toxicol. Pathol*. **1**: 23–26

Miller-Larsson, A., Mattsson, H., Hjertberg, E., Dahlbäck, M., Tunek, A., Brattsand, R. (1998) Reversible fatty acid conjugation of budesonide. Novel mechanism for prolonged retention of topically applied steroid in airway tissue. *Drug Metab. Dispos*. **26**: 623–630

Rau, K., Singh, R., Goldberg, E. (2002) Synthesis and characterization of cross-linked silicone thin films by pulsed laser ablation deposition (PLAD). *Mater. Res. Innov*. **5**: 162–169

Silverstein, R. M., Webster, F. X. (1991) *Spectrometric identification of organic compounds*. John Wiley and Sons, New York

Sodergard, A., Stolt, M. (2002) Properties of lactic acid based polymers and their correlation with composition. *Prog. Polym. Sci*. **27**: 1123–1163

Srinivasan, R., Braren, B. (1989) Ultraviolet laser ablation of organic polymers. *Chem. Rev*. **89**: 1303–1316

Srinivasan, R., Mayne-Banton, V. (1982) Self-developing photoetching of poly(ethylene terephthalate) films by far-ultraviolet excimer laser radiation. *Appl. Phys. Lett* **41**: 576–578

Suarez, S., Gonzalez-Rothi, R. J., Schreier, H., Hochhaus, G. (1998) Effect of dose and release rate on pulmonary targeting of liposomal triamcinolone acetonide phosphate. *Pharm. Res*. **15**: 461–465

Suzuki, N., Makino, T., Yamada, Y., Yoshida, T., Onari, S. (2000) Structures and optical properties of silicon nanocrystallites prepared by pulsed-laser ablation in inert background gas. *Appl. Phys. Lett*. **76**: 1389–1391

Talton, J., Fitz-Gerald, J., Singh, R., Hochhaus, G. (2000) Nano-thin coatings for improved lung targeting of glucocorticoid dry powders: in vitro and in-vivo characteristics. *Resp. Drug Deliv*. **7**: 67–74

Thomson, D. C. (2004) Pharmacology of therapeutic aerosols. In: Hickey, A. J. (ed) *Pharmaceutical inhalation aerosol technology*. Marcel Dekker, Inc., New York, pp 31–64